A&A 519, A58 (2010)
DOI: 10.1051/0004-6361/200913254

Astronomy & Astrophysics

Horizontal supergranule-scale motions inferred from TRACE ultraviolet observations of the chromosphere

H. Tian[1], H. E. Potts[2], E. Marsch[3], R. Attie[3], and J.-S. He[3]

[1] School of Earth and Space Sciences, Peking University, Beijing, PR China
e-mail: tianhui924@pku.edu.cn
[2] Department of Physics and Astronomy, University of Glasgow, G12 8QQ Glasgow, UK
e-mail: hugh@astro.gla.ac.uk
[3] Max-Planck-Institut für Sonnensystemforschung, Katlenburg-Lindau, Germany
e-mail: marsch@mps.mpg.de

Received 7 September 2009 / Accepted 2 June 2010

ABSTRACT

Aims. We study horizontal supergranule-scale motions revealed by TRACE observation of the chromospheric emission, and investigate the coupling between the chromosphere and the underlying photosphere.
Methods. A highly efficient feature-tracking technique called balltracking has been applied for the first time to the image sequences obtained by TRACE (transition region and coronal explorer) in the passband of white light and the three ultraviolet passbands centered at 1700 Å, 1600 Å, and 1550 Å. The resulting velocity fields have been spatially smoothed and temporally averaged in order to reveal horizontal supergranule-scale motions that may exist at the emission heights of these passbands.
Results. We find indeed a high correlation between the horizontal velocities derived in the white-light and ultraviolet passbands. The horizontal velocities derived from the chromospheric and photospheric emission are comparable in magnitude.
Conclusions. The horizontal motions derived in the UV passbands might indicate the existence of a supergranule-scale magneto-convection in the chromosphere, which may shed new light on the study of mass and energy supply to the corona and solar wind at the height of the chromosphere. However, it is also possible that the apparent motions reflect the chromospheric brightness evolution as produced by acoustic shocks which might be modulated by the photospheric granular motions in their excitation process, or advected partly by the supergranule-scale flow towards the network while propagating upward from the photosphere. To reach a firm conclusion, it is necessary to investigate the role of granular motions in the excitation of shocks through numerical modeling, and future high-cadence chromospheric magnetograms must be scrutinized.

Key words. Sun: photosphere – Sun: chromosphere – Sun: UV radiation – Sun: granulation – solar wind

1. Introduction

Quasi-steady convective flows of different scales have been suggested to play an important role in the processes of mass supply and energy transport across different layers of the solar atmosphere (e.g., Foukal 1978; Krijger et al. 2002; Marsch et al. 2008; Dammasch et al. 2008; Curdt et al. 2008). As is well known, granulation with a typical 1-Mm size and 5-min lifetime are ubiquitous in high-resolution photospheric images (e.g., Title et al. 1989; Berrilli et al. 2002; Jin et al. 2009). Groups of theses granules tend to move in a systematic way, which is characterized by a cellular convective motion at scales of the order of 32 Mm (Leighton et al. 1962). This larger-scale flow was termed supergranulation, with cells of which the boundaries coincide with the chromospheric network and lanes of magnetic concentrations (e.g., Leighton et al. 1962; Simon & Leighton 1964; Simon et al. 1988; Wang & Zirin 1988).

Under the assumption that the granules can be considered as tracers of the underlying larger-scale velocity fields (Simon et al. 1988; Rieutord et al. 2001) of magnetoconvection, one can derive the related horizontal flow speed by the widely used LCT (Local correlation tracking) technique (November & Simon 1988). Recently, Potts et al. (2004) developed a new method for tracking flow fields. This so called balltracking method is more noise-tolerant and highly efficient for analysing large data sets. The flow field inferred by this method has a similar accuracy to that obtained by LCT.

The horizontal motions in the chromosphere have not been scrutinized and are not understood well. Few attempts have been made to measure chromospheric proper motions, e.g., by applying LCT to the Hα images obtained in active regions (Yi & Molowny-Horas 1995; Chae et al. 2000; Yang et al. 2003). By using this method, the typical horizontal velocity in the chromospheric network was found to be 1000–1500 m/s (Yi & Molowny-Horas 1995). However, the small-scale structures present in Hα images appear to be elongated and thus are different from the cellular-shaped granules. Moreover, the Hα line is very sensitive to and strongly influenced by dynamic events. Thus, the explanation of the horizontal velocities as measured from Hα images is not straightforward.

Besides Hα, the Ca II H & K lines have also been extensively used to explore dynamics in the chromosphere. The chromospheric network, which coincides with the magnetic network and outlines the supergranular boundaries, is the most prominent structure on images of Ca II, while the cell interiors (internetwork regions) which are enclosed by the network occupy most of the quiet-Sun area. Internetwork areas are filled with intermittent grainy brightenings. These emission features are usually termed $H(K)_{2v}$ cell grains because their intensities peak dramatically

just blueward of the Ca II H & K line centers. These internetwork grains (or cell grains) are also present on wider-band (a few Å) Ca II filtergrams, but at a lower contrast and a slight phase shift (Rutten et al. 1999a,b). The sizes of internetwork grains are about 1−4 Mm, and their lifetimes are usually less than 12 min (Rutten & Uitenbroek 1991; Tritschler et al. 2007). For a detailed review of the Ca II H_{2v} & K_{2v} cell grains, we refer to Rutten & Uitenbroek (1991).

By comparing the quiet-Sun images obtained by TRACE (transition region and coronal explorer, Handy et al. 1999) in its three ultraviolet (UV) passbands (centered at 1700 Å, 1600 Å, and 1550 Å) and a co-temporal Ca II K filtergram, Rutten et al. (1999a) found a high degree of spatial agreement between the Ca II K image and the TRACE images, in particular the 1700 Å one. They concluded that the three TRACE channels portray internetwork grain phenomena as well as Ca II K filtergrams do. Therefore, TRACE image sequences provide an excellent means to study the dynamics of internetwork grains (Rutten et al. 1999a).

By applying here the balltracking technique for the first time to the TRACE images obtained in the passband of white light and the three UV passbands centered at 1700 Å, 1600 Å, and 1550 Å, we have made an attempt to study horizontal photospheric and chromospheric motions in a large area of the quiet Sun. Our analysis revealed a striking correlation between the horizontal velocities derived in the white-light passband and the UV passbands, a finding which might shed new light on our understanding of mass supply to the corona and solar wind. Alternatively, our finding may provide insights into the excitation and propagation of the shock sequences which might produce the bright internetwork grains.

2. Data analysis and results

The TRACE image sequence analysed here was obtained on 14 October 1998 from 08:20 to 09:30 UTC in a quiet-Sun region around disk center. Images in the four passbands as mentioned above were taken with a cadence of 21 s. The sizes of the images are 512 × 512 pixels squared, with a pixel size of 0.5″.

The standard software for reducing TRACE data was applied to this data set, including the removal of cosmic rays, subtraction of dark currents, normalization of the counts, and so on. Then we used the IDL procedure *Rot_XY.pro* available in *SolarSoft* to take into account the solar rotation effect. The satellite jitter was subsequently removed with an accuracy of 0.025″, by applying the cross-correlation technique to enlarged (by a factor of 20) images. For computational efficiency, we resampled the data to obtain a cadence of 42 s, and then extracted a sub-region with a size of 200″ × 200″ from the coaligned images.

Each image was spatially Fourier filtered to remove solar oscillations and observational noise and thus to remove the large scale variations, as described in Potts et al. (2004). In addition, the 1700 Å, 1600 Å, and 1550 Å images have the problem that the intensity variation is very non-linear, with a small number of very bright points that tend to dominate the filtered data. These data were scaled by raising the intensity to a power of 0.4 to compress the intensity data into a more uniform range, before filtering. We kept the Fourier components with wavelength between 1″ (the minimum measurable wavelength) and 3.5″ (upper limit of the granule/grain size). Figure 1 presents the first images of the sequences taken with the passbands of white light and 1700 Å. It is clear from the figure that the size of the chromospheric grains inside cell interiors is comparable to that of the photospheric grains. The brightness range of the cell grains seems to be larger than that of the photospheric grains. The most prominent difference between the photospheric emission and the chromospheric emission is the much more enhanced network emission in the chromosphere. But the network bright points only constitute a minor part of the area, and thus their contribution to the tracked velocities is minor. Figure 1 also shows the corresponding filtered images, which reveal clearly that both the dark and bright points inside the cell interiors are comparable in size (or width).

In the balltracking technique as developed by Potts et al. (2004), one considers a photospheric image in a three-dimensional representation by regarding the brightness as corresponding to a geometrical height. Small floating balls are dropped on to this surface and tend to settle in the local minima between some adjacent granules. As the granulation pattern evolves, the balls will be pushed around and thus follow and reveal the motion of the granules. It has been demonstrated that the results from this method have an accuracy similar to those produced by LCT (Potts et al. 2004). This method has been successfully applied to high-resolution continuum images obtained by MDI/SOHO (Potts et al. 2007; Potts & Diver 2008; Innes et al. 2009) and SOT/Hinode (Attie et al. 2009).

As mentioned by Potts et al. (2004), the balltracking method is not limited to flows in the photosphere, but will also work for any velocity field in which there are visible moving features of known scale length. Here we made the first attempt to apply this method to TRACE images in the passband of white light and several UV passbands. We set the radius of the tracking ball at 1.2″. As described in Attie et al. (2009), the output of the balltracking procedure are velocity fields derived from the displacements of many individual tracking balls, which reflect the fast and stochastic small-scale granular motions. To extract the underlying large-scale velocity field the data needs to be spatially smoothed and temporally averaged. Rieutord et al. (2001) suggested that the velocity field may not be faithfully described by granular motions at spatial scales less than 2.5 Mm, or at temporal scales shorter than half an hour. Our tracking results have been smoothed over 3.5 Mm and running-averaged over the entire 70 min. The tracking routine actually tracked the data twice, once with the normal data and once with the inverted data, and gave very similar results in both cases. We took the average of the two results. The error estimate for the tracking was obtained from the difference of these two results. The root mean square values of the errors are well below those of the tracked velocities in all of the four passbands.

Finally, since the velocity values obtained by balltracking are usually underestimated as compared to the true velocities (Potts et al. 2004), we need to divide the balltracked velocities by a scaling factor. Starting with the de-rotated and jitter-removed data cube, we chose a sub-area from the first frame of the data, and offset each subsequent frame in turn by a small distance, representing an additional imposed velocity. Four velocities were chosen to produce four offset data cubes, which were then tracked using balltracking. By applying a linear fit to the mean velocity derived from each offset data cube versus the offset velocity, we obtained a scaling factor in each passband. The derived velocities were divided by this value. Figure 2 shows the result of the fitting in each passband. The values of the slopes are used as velocity calibration factors.

The distributions of the resulting velocities are presented in Fig. 3. It turns out that the velocity values are comparable in different passbands. The median values of the derived velocities are 247 m/s, 258 m/s, 258 m/s, and 284 m/s, in the

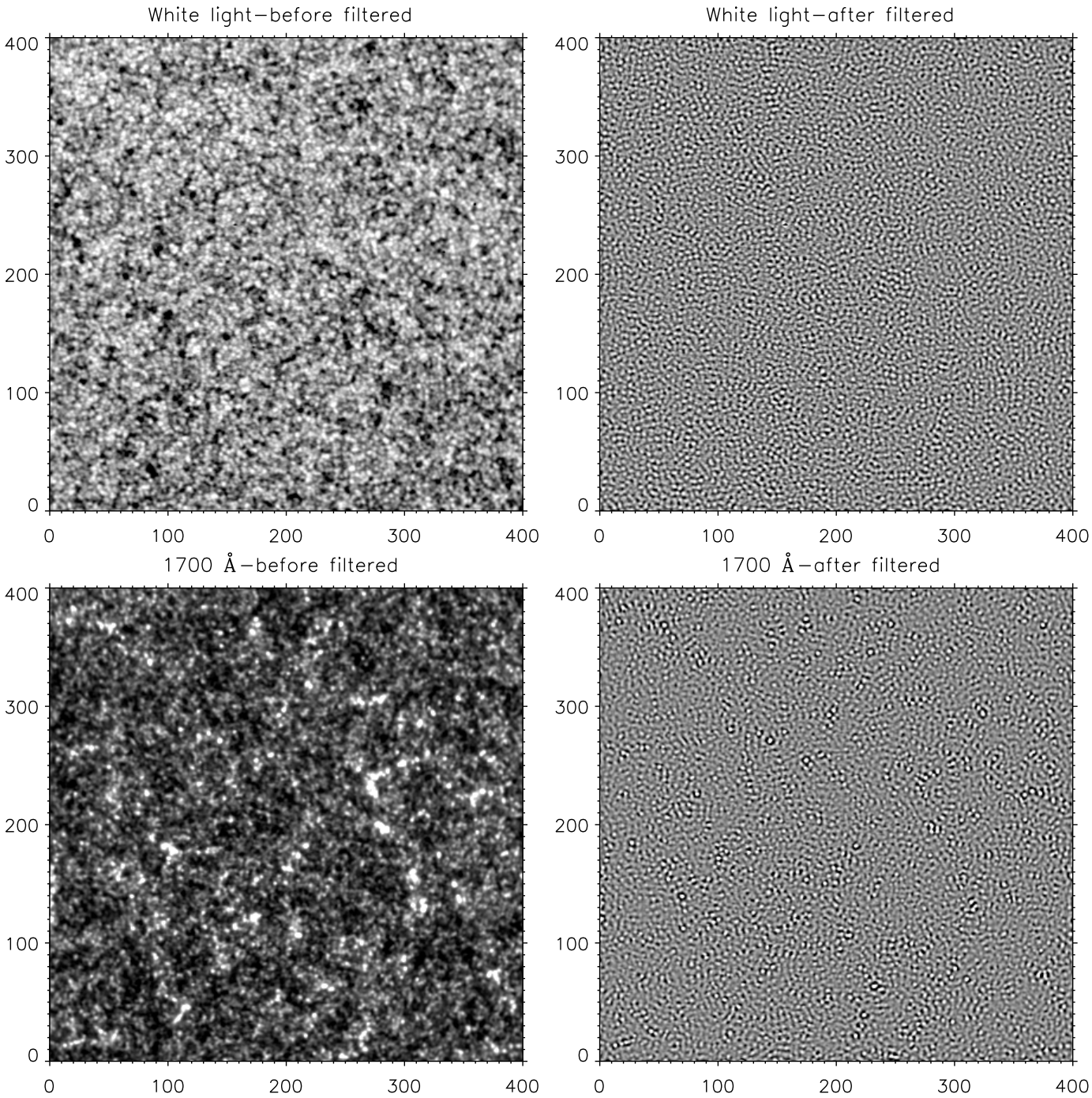

Fig. 1. Images taken at 08:20 in the passbands of white light (*upper*) and 1700 Å (*lower*). The original and filtered images are presented on the *left* and *right*, respectively. The size of each image is 200″ × 200″.

passbands of white light, 1700 Å, 1600 Å, and 1550 Å, respectively. Following the method in Potts et al. (2004), we estimated an uncertainty of 29 m/s for the velocity measurement.

Figure 4 presents the velocity fields for the four passbands. The cell boundaries, which were calculated by applying the automatic recognition algorithm developed by Potts & Diver (2008) to velocities obtained in the corresponding passband, are shown as the background (lanes). A direct comparison of the cell boundaries as calculated from the velocity field in white light and from that in the passband of 1700 Å with the 1700 Å intensity image was made and is shown in Fig. 5.

We also calculated the linear Pearson correlation coefficients of each component of the velocity field as well as the velocity magnitude, between each pair of passbands. The results are listed in Table 1. The average correlation coefficients of the unfiltered intensity images between each pair of passbands are also listed therein.

3. Supergranular horizontal flows in the photosphere

Photospheric horizontal flows have been extensively investigated through ground based observations. Image sequences obtained by the TRACE satellite are suitable for motion tracking in the photosphere as they offer long uninterrupted runs over large areas (up to 512″ × 512″) with no seeing problems. The spatial

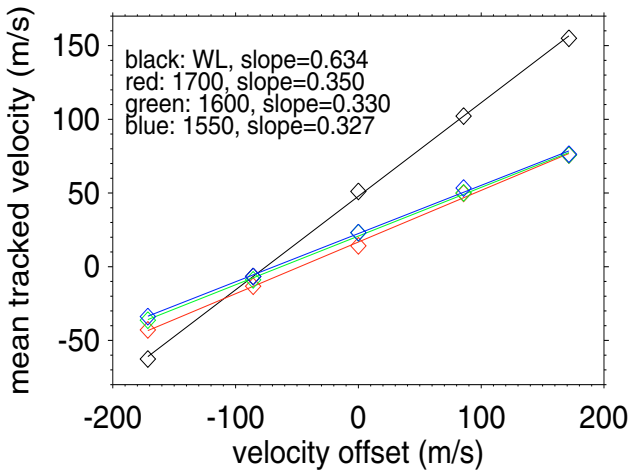

Fig. 2. Calibration factors obtained by a linear fit to the mean velocity derived from each offset data cube versus the offset velocity, in the passbands of white light (black), 1700 Å (red), 1600 Å (green), and 1550 Å (blue). The values of the slopes are used as velocity calibration factors.

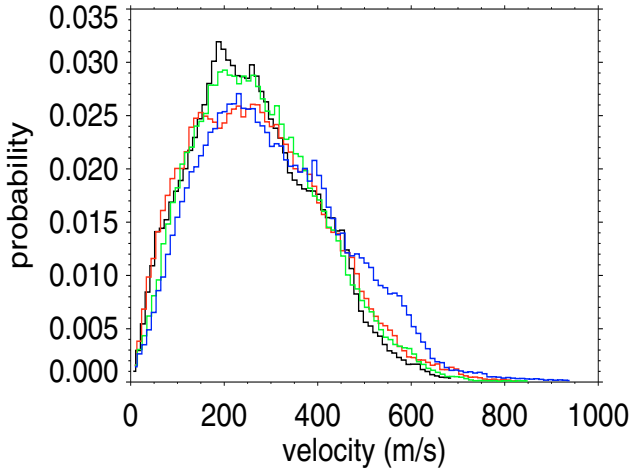

Fig. 3. Histogram of the measured horizontal velocities in the passbands of white light (black), 1700 Å (red), 1600 Å (green), and 1550 Å (blue).

Table 1. The linear Pearson correlation coefficients of the intensity (I), two components of the velocity field (v_x and v_y), as well as the velocity magnitude (v) between each pair of passbands.

Passbands	I	v_x	v_y	v
WL/1700	0.13	0.63	0.71	0.35
WL/1600	0.09	0.58	0.62	0.26
WL/1550	0.06	0.50	0.61	0.22
1700/1600	0.96	0.81	0.81	0.63
1700/1550	0.82	0.73	0.71	0.48
1550/1600	0.92	0.78	0.81	0.61

resolution of 1″ is just high enough to resolve the granular structure.

By applying the balltracking technique to white light images observed by TRACE, we have reconstructed the well-known photospheric supergranular flow pattern in a quiet-Sun region with a size of 200″ × 200″. From Fig. 5 we find that the calculated cell boundaries generally match the network pattern as seen in the 1700 Å image. In the 1700 Å image, there are still a few segments of the bright lanes which are not reproduced from these calculations. It might be due to the effect of temporal variation, height variation, UV contamination of the white-light emission, smoothing and averaging of the tracking results, or the fact that small granules below the detection limit of TRACE can not be traced properly.

The velocity magnitude in white light is consistent with the results in Krijger et al. (2002) and Attie et al. (2009), but smaller than those in Wang et al. (1995) and Roudier et al. (1999). This should be the result of the different smoothing and averaging of the tracked velocity fields. As mentioned in Attie et al. (2009), a weaker smoothing and averaging will increase the velocity values. Our choice of the smoothing and averaging scales is a compromise between a more accurate velocity measurement and a higher resolution to distinguish flows with sharp gradient.

Krijger et al. (2002) applied the LCT technique to a TRACE white-light image sequence in a small region, and concluded that it is possible to use the TRACE observations to measure photospheric horizontal velocity fields. Here we have demonstrated that the supergranular flow pattern in the photosphere can be recovered by applying the highly efficient balltracking method to the white-light images observed by TRACE in a large area of the quiet Sun.

4. Horizontal motions revealed through the chromospheric emission

As mentioned previously, the horizontal flow field in the chromosphere has not been understood well. Only a few attempts have been made to measure chromospheric proper motions by applying LCT to Hα images obtained in active regions (Yi & Molowny-Horas 1995; Chae et al. 2000; Yang et al. 2003). The TRACE observations allow a direct comparison of possible large-scale horizontal motions in the chromosphere with those in the underlying photosphere.

From Fig. 4 we can see that the velocity fields obtained in the three UV passbands also show cell structures which are similar to those in the white-light passband. The diverging flow-like patterns in some cells are highly coincident in different passbands. The correlation coefficients listed in Table 1 are large, again indicating a high correlation between the derived horizontal motions in different passbands. The cell boundaries calculated from the velocity field in the 1700 Å passband also coincide more or less with the chromospheric network, as shown in Fig. 5. According to our knowledge, this is the first time that supergranulation-scale horizontal motions, both in and above the photosphere, are revealed in a large area of the quiet Sun.

4.1. Formation height of emission from TRACE UV filters

According to Handy et al. (1999) and Worden et al. (1999), the emission in the 1700 Å passband ($4-10 \times 10^3$ K) is UV continuum originating around the temperature minimum; the emission in the 1600 Å passband ($4-10 \times 10^3$ K) has contributions from the UV continuum and several lines like Fe II and C I, but the dominant contributor is the UV continuum from the region of temperature minimum. According to the VAL-C solar atmosphere model (Vernazza et al. 1981), the temperature minimum region is located at about 500 km above $\tau_{500} = 1$, corresponding to the upper photosphere/lower chromosphere (Worden et al. 1999; Rutten & Krijger 2003; McAteer et al. 2004).

The emission from the 1550 Å passband is mainly a combination of C IV and the underlying UV continuum emission (Handy et al. 1999; Worden et al. 1999). As mentioned in

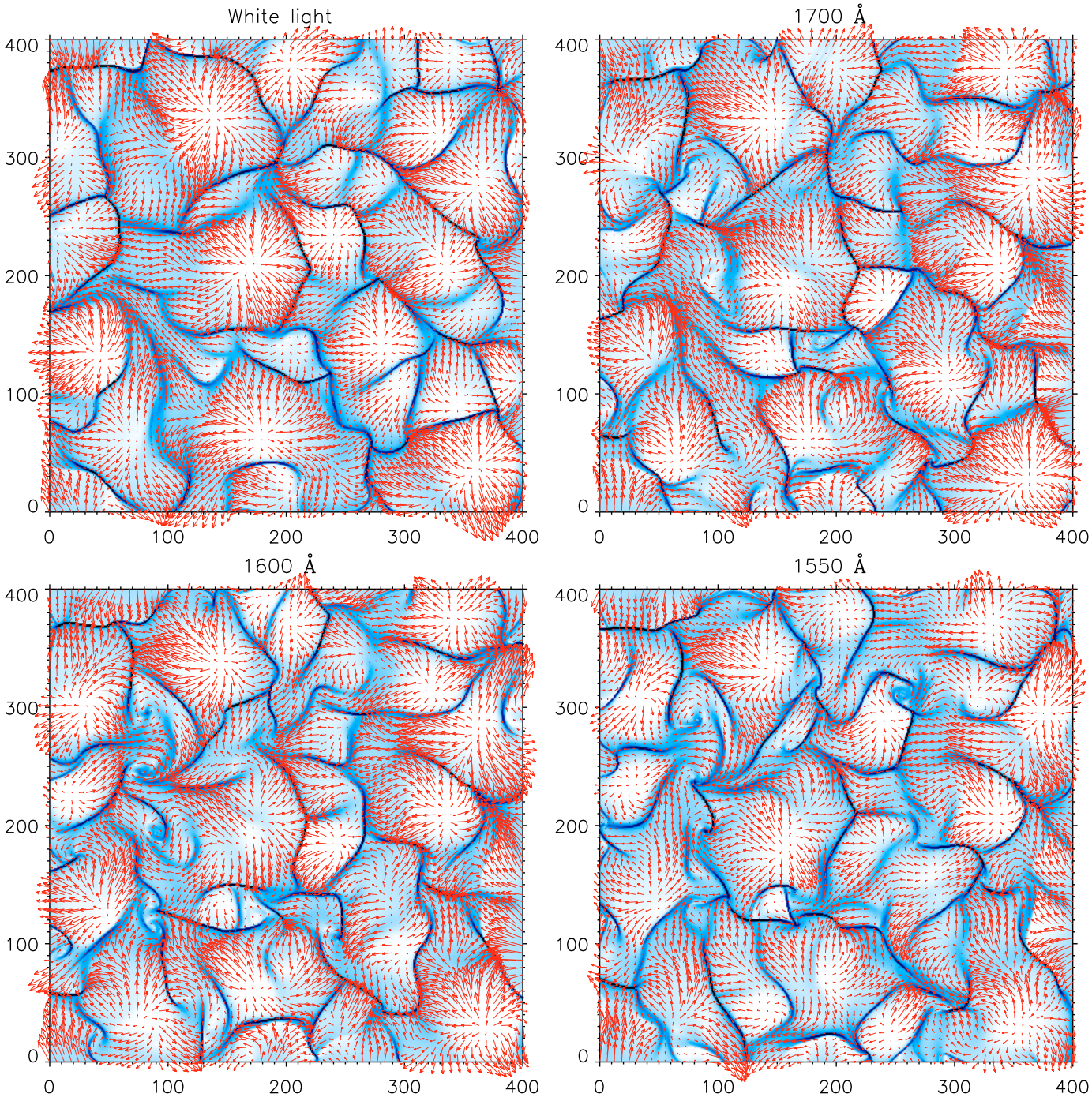

Fig. 4. Velocity vector fields as calculated by using the image sequence in the passband of white light (*upper left*), 1700 Å (*upper right*), 1600 Å (*lower left*), and 1550 Å (*lower right*). The lanes represent cell boundaries as calculated from the velocity field in the corresponding passband. The size of each image is 200″ × 200″.

Krijger et al. (2001) and Rutten et al. (1999a), the C IV lines dominate the emission of the 1550 Å passband in active regions, while in the quiet Sun contributions from the UV continuum and several weak lines (e.g. C I lines) dominate in the 1550 Å passband. Handy et al. (1999) mentioned that the 1550 Å image resembles an image taken in the center of the Ca II K line with a bandpass of a few Angstroms. So the major contributor to the emission of the 1550 Å passband seems to be the UV continuum, and thus the 1550 Å passband should be dominated by the chromospheric emission.

Similar to many papers such as Krijger et al. (2001) and McAteer et al. (2004), we use the term "chromosphere" even for the upper photosphere since images of the TRACE UV passbands largely differ from the photospheric images and essentially sample the chromospheric network. We realize that there are limitations to assigning the height of formation to emission from the broad band-pass filters on the TRACE UV channels. However, by comparing the quiet-Sun images obtained by TRACE in three UV passbands (centered at 1700 Å, 1600 Å, and 1550 Å) and a co-temporal Ca II K filtergram,

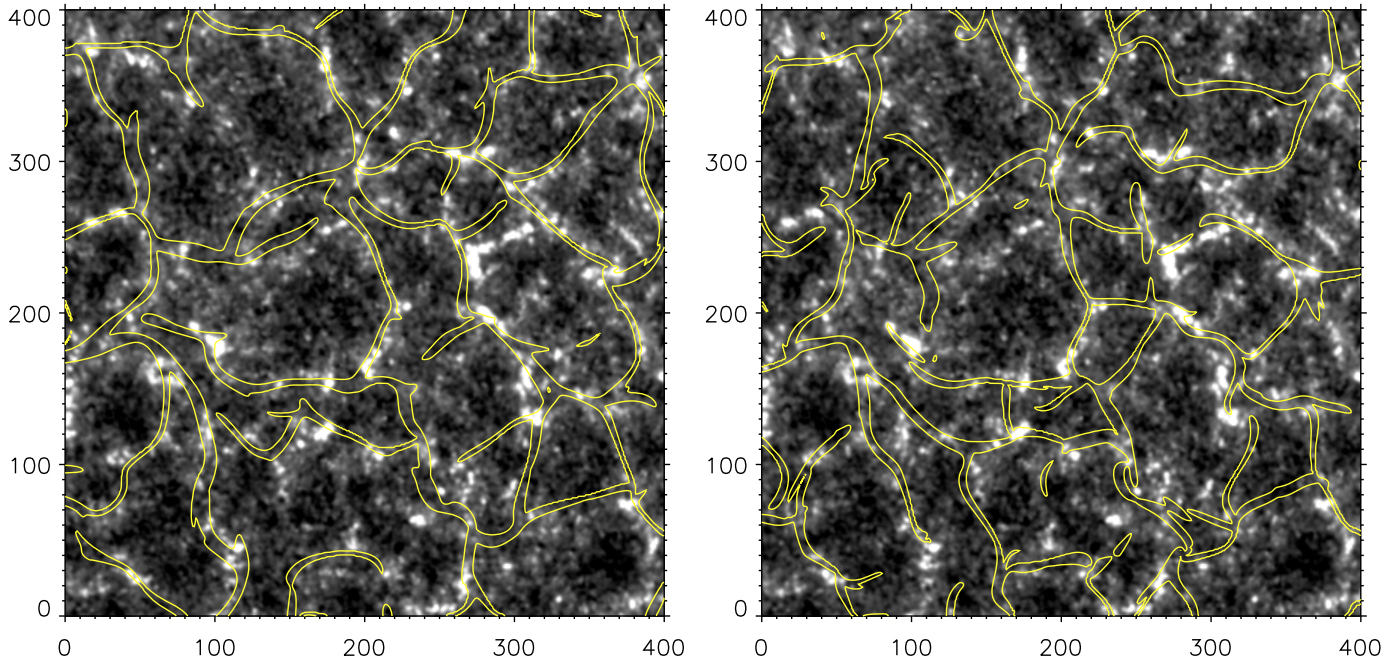

Fig. 5. The yellow lanes representing cell boundaries as calculated from the velocity field in white light (*left*) and from that in the passband of 1700 Å (*right*) are superposed on the averaged intensity image in the 1700 Å passband. The size of the image is 200″ × 200″.

Rutten et al. (1999a) concluded that there is a high degree of spatial correspondence between the Ca II K image and the TRACE images, and that the three TRACE channels reveal internetwork emission features as well as Ca II K filtergrams do. Similar conclusion was also reached by Handy et al. (1999). Thus, we believe that the structures visible on the TRACE UV filters are well formed at a certain height, probably the lower part, of the chromosphere.

The cross-talk (overlap) between emission from different passbands might also influence our results. First, since our data were obtained shortly after TRACE was launched, the transmission curves of UV passbands presented in Fig. 9 of Handy et al. (1999) should have not changed too much, and thus the leaking of the white-light signal into the UV emission should be marginal. Second, there is a large part of overlap between emission of the 1700 Å and 1600 Å passbands, which accounts for the very large correlation between velocities in the two passbands. This overlap does not change our conclusion, since our main finding is the correlation between velocities in the white-light and UV passbands, not the correlation between two UV passbands. Third, the UV contamination of the white-light emission might not be trivial and is likely to be one of the reasons why some bright chromospheric network lanes are not reconstructed by the calculated cell boundaries. This is, however, counteracted by a higher correlation between the velocities than the intensities.

4.2. Nature of internetwork grains

Internetwork grains (or cell grains) have been extensively studied through ground based observations using Ca II H & K lines (for a review, see Rutten & Uitenbroek 1991). As mentioned above, Rutten et al. (1999a) found a high degree of spatial correspondence between the Ca II K image and the TRACE UV images (passbands of 1700 Å, 1600 Å, and 1550 Å). They concluded that the three TRACE channels portray internetwork grain phenomena as well as Ca II K filtergrams do.

Internetwork regions occupy most of the quiet Sun area. So with the balltracking technique we are mainly tracking the motions of the internetwork grains in TRACE UV filters. Before interpreting the observed horizontal motions in the chromosphere, we need to understand the nature of these internetwork grains.

In fact, there are long-lasting disputes on this issue. Direct evidence for the spatial correspondence between the cell grains and internetwork magnetic elements (Livingston & Harvey 1975) was provided by Sivaraman & Livingston (1982). The magnetic origin of the cell grains was further confirmed by Damé et al. (1984), Damé (1985), Damé & Martic (1987), Damé & Martic (1988), Sivaraman (1991), and Sivaraman et al. (2000). Based on *Hinode* observations, de Wijn et al. (2008) found that some of the magnetic elements are associated with the chromospheric cell grains. Recently, although no obvious correlation between the magnetic flux density and the Ca II H internetwork brightness was obtained, Yang et al. (2009) **were** still inclined to believe that there should be a correlation between the two, and they attributed the lack of correlation to the low cadence of Ca II H images they used.

However, others doubt this conclusion. And through observations and modelings they believe that the occurrence of internetwork grains does not depend on magnetism but is caused by weak acoustic shocks which propagate upwards through the low chromosphere (Rutten & Uitenbroek 1991; Remling et al. 1996; Carlsson & Stein 1997; Lites et al. 1999; Loukitcheva et al. 2009). Worden et al. (1999) compared the cell grains observed in TRACE UV passbands and the corresponding photospheric magnetic field, and suggested that the internetwork magnetic field is essentially uninvolved with the production of cell grains in the 1600 Å passband, but could have a small involvement with the cell grains in the 1216 Å (Lyα) passband.

Brandt et al. (1992, 1994) found that there are two types of cell grains: (i) oscillatory K_{2v} flashers, appear only a few times with a modulation of 3-min oscillation, brief spatial memory, 5−10 grains per cell; (ii) persistent K-line grains, retaining long-term identity while traveling through the cell, flashing with 3−5 min periodicity, about 1 grain per cell. The short-living grains were suggested to be generated by acoustic shocks and have nothing to do with the magnetic field. On the contrary, a spatial correspondence between internetwork magnetic features and persistent flashers was observed. The persistent flashers probably represent the chromospheric signatures of newly-emerged strong-field ephemeral regions on their ways to be part of the network. This finding was confirmed by Nindos & Zirin (1998). Lites et al. (1999) also found persistent flashers but pointed out that they are very rare. While with UV image sequences obtained by TRACE, Krijger et al. (2001) identified many such long-living features, and McAteer et al. (2004) also found that ∼50% cell grains are persistent flashers. Persistent flashers were called internetwork bright points by de Wijn et al. (2005), in which they were suggested to correspond to the strongest internetwork magnetic elements.

The question of whether or not the chromospheric cell grains are correlated with the magnetic flux in internetwork regions is very important to study the chromospheric heating and dynamics. Here we don't intend to answer whether or not the magnetic field plays a role, or a major role, in the production of chromospheric cell grains, since there are still debates on this issue and it is not so easy to distinguish between the two possibilities. As pointed out by Kamio et al. (2006), we need more detailed observations to solve this problem. Instead, we discuss the implications of our results and point out directions of future studies, with respect to each of the two suggested natures of cell grains.

4.3. Magneto-convection in the chromosphere

As shown in Fig. 4, the measured horizontal velocity fields in the chromosphere and photosphere show a similar supergranule-scale cell-like pattern, which prompts us to think if they represent an upward extension of supergranular horizontal flows to the chromosphere.

The idea that supergranular flows may penetrate into higher layers has already been suggested by several authors. It is known that motions of granules in the photosphere follow the supergranulation plasma flows because these plasma flows are observed in Doppler shift. In the middle chromosphere (formation height of Si II λ1817), such Doppler shift was also investigated and demonstrated to be existing (November et al. 1979). November et al. (1979) even predicted that supergranular velocities should be evident in the TR. November et al. (1982) found that large-scale patterns of up- and downflows in the middle chromosphere correlate well with those seen in the photosphere and concluded that vertical flows of supergranular scale appear to extend into the chromosphere. Height variation of the velocity field in the photosphere has also been studied. Observations by Deubner (1971) indicated that the vertical motions increase with height, and that the horizontal supergranular flow decreases slightly, in the photosphere from the formation height of C I λ5380 to that of Mg I λ5173. The latter is formed at the temperature minimum (upper photosphere/lower chromosphere) (November et al. 1982; November 1989). Giovanelli (1980) found that the supergranular horizontal velocities show no significant variation with height over the range of formation of C I λ9111, Fe I λ8688, and Mg I λ8806, but there is a substantial reduction to about one-half of this at the level of Ca II λ8542. More recently, Del Moro (2007) investigated the 3D photospheric velocity field of a supergranular cell, and proposed that large flow features can penetrate into the upper photosphere.

Simon & Leighton (1964) suggested that the supergranulation flow field carries the internetwork magnetic field to cell boundaries, forming the pattern of the chromospheric network. So far many observations have confirmed that most internetwork magnetic elements move toward the boundaries of the magnetic network (e.g., Martin 1988; Simon et al. 1988; Wang & Zirin 1988; Zhang et al. 1998). Using magnetograms obtained by the Big Bear Solar Observatory (BBSO), Zhang et al. (2006) estimated the emergence rate of the new flux (ephemeral regions) to be $\sim 5 \times 10^{-19}$ cm^{-2} day^{-1} in the quiet Sun. Wang et al. (1995) calculated the mean area of internetwork magnetic elements, which is about $10''^2$. Then the mean size and height of an internetwork magnetic element should be about $3''$. According to Vernazza et al. (1981), the temperature minimum, which marks the boundary between the photosphere and chromosphere, is located at 500 km above $\tau_{500} = 1$. So in the internetwork regions, there should be a large number of magnetic elements which extend above the photosphere. And when these internetwork magnetic elements are swept by the supergranular flows to the magnetic network, we should see the horizontal motions of their footpoints and apices in the photosphere and chromosphere, respectively. Unfortunately, high-quality magnetograms of the quiet Sun above the photosphere are still difficult to obtain. Thus, currently it is difficult to validate the existence of these strong internetwork magnetic elements above the photosphere. However, in an active region Lin et al. (2006) found a correlation between localized emission enhancement above the photosphere (in the chromosphere and TR) and a moving magnetic feature, which followed the boundary of a supergranulation cell. Zhang & Zhang (2000) analyzed quiet-Sun photospheric and chromospheric magnetograms observed by the vector video magnetograph at Huairou Solar Observing Station, and found that all visible variations in the photosphere had corresponding variations in the chromosphere, although the Hβ line, which they used to derive the chromospheric magnetogram, are complicated and may include signals from both the photosphere and chromosphere. Solanki et al. (2003) observed a set of rising magnetic loops and found that magnetic signatures of the loop legs are clearly present in the magnetogram of the upper chromosphere. Recently, based on Hinode observations, Shimojo & Tsuneta (2009) even found a clear correlation between coronal activities and photospheric minority magnetic polarities in the polar coronal hole. All these observations seem to suggest that horizontal movements of internetwork magnetic elements should reveal horizontal motions both in and above the photosphere.

If the chromospheric internetwork grains have a one-to-one correspondence to enhanced magnetic fields (Sivaraman & Livingston 1982; Damé et al. 1984; Damé 1985; Damé & Martic 1987, 1988; Sivaraman 1991; Sivaraman et al. 2000), or the persistent flashers which are related to strong internetwork magnetic elements (Brandt et al. 1992, 1994; Nindos & Zirin 1998; Krijger et al. 2001; McAteer et al. 2004; de Wijn et al. 2005) play a dominant role in the chromospheric internetwork emission, the velocity fields revealed by TRACE UV observations naturally represent the horizontal component of magneto-convection in the chromosphere. By comparing the velocity fields obtained in white light with those in the three UV passbands, we can conclude that the supergranular pattern does not completely disappear above the photosphere. The diverging flows in some cells are still very clearly seen in the chromosphere. Some supergranular motions are extending into the overlying formation layers

of the 1700 Å, 1600 Å, and 1550 Å emission. The comparable velocities derived in the photosphere and chromosphere are also easy to understand because they reflect horizontal motions of the same features, although at different heights.

The existence of a supergranule-scale magneto-convection in the chromosphere may shed new light on the study of mass and energy supply to the corona and solar wind at the height of the chromosphere. It is believed that part of the magnetic network flux opens into the corona in the shape of funnels, whilst the rest of the network consists of a dense population of low-lying loops with lengths less than 10^4 km and varying orientations (Dowdy et al. 1986; Marsch & Tu 1997; Peter 2001). Magnetic loops reaching to the height of the chromosphere and TR can be swept by the supergranular flow from the cell interior to its boundaries, where they can interact with magnetic funnels, and by reconnection may supply mass and energy to the funnels (Axford et al. 1999; Aiouaz et al. 2005; Aiouaz 2008; He et al. 2007; McIntosh et al. 2007; Tian et al. 2008a, 2009). Reconnection at the interface between cool side loops and the network flux tubes may occur in the chromosphere and TR, resulting in the solar wind outflow (Tu et al. 2005; He et al. 2008; Büchner & Nikutowski 2005; Tian et al. 2008b, 2010) or upflows along loop legs (Tian et al. 2008a, 2009), and downflows at lower layers. Thus, horizontal motions representing supergranule-scale magneto-convection in the chromosphere and TR are vital in such processes as mass supply and energy delivery to the corona and solar wind through funnels. Our finding may represent the observational evidence for these motions.

However, we should point out that the extension of strong magnetic elements into the chromosphere can only be explicitly confirmed when the magnetic field above the photosphere can be accurately measured, and that the existence of such supergranule-scale magneto-convection in the chromosphere can only be confirmed by following the evolution of the chromospheric magnetic field with high cadence and high resolution.

4.4. Chromospheric brightness evolution induced by photospheric granular motions

As mentioned above, some authors doubt the magnetic origin of the chromospheric cell grains, but believe that cell grains are caused by weak acoustic shocks which propagate upwards through the low chromosphere (Rutten & Uitenbroek 1991; Remling et al. 1996; Carlsson & Stein 1997; Loukitcheva et al. 2009). Lites et al. (1999) confirmed the existence of magnetism-related grains but pointed out that they don't play a dominant role in the chromospheric internetwork emission. If most cell grains are indeed of acoustic origin, then the horizontal motions we derived by using TRACE UV observations are likely to represent chromospheric brightness evolution induced by the shocks.

In the one-dimensional simulation of Carlsson & Stein (1997), a piston located at the bottom of the computational domain (100 km below $\tau_{500} = 1$) drives waves through the atmosphere, then propagating waves near or just above the acoustic cutoff frequency interfering with higher frequency waves that induce them to steepen rapidly and form shocks near 1 Mm above $\tau_{500} = 1$. The chromospheric shocks produce a large source function, yielding the high emissivity of internetwork grains. If this scenario is correct, it is essential to investigate the horizontal distribution of pistons at the bottom layer, which was not addressed in the simulation of Carlsson & Stein (1997) due to its one-dimensional restriction.

Several attempts have been made to investigate this issue. As pointed out by Rutten et al. (1999b), turbulent convection seems to supply the pistons that excite shock sequences and produce the cell grains. Rimmele et al. (1995) found that enhanced acoustic wave activities, the so-called "acoustic events", occur preferentially in dark intergranular lanes. This spatial correspondence was later confirmed by Goode et al. (1998) and Strous et al. (2000). Hoekzema & Rutten (1998) and Hoekzema et al. (1998) further pointed out that dark intergranular lanes tend to show excess ~3-min waves in the photosphere. These transient acoustic waves are suggested to be excited by small granules that undergo a rapid collapse (Rast 1999; Skartlien et al. 2000).

The relationship between enhanced wave activities in the photosphere and enhanced chromospheric emission was also investigated by several authors. For example, through wavelet analyses, Kamio et al. (2006) found that the occurrence of chromospheric brightenings is correlated with enhanced 5 mHz velocity oscillations in the chromosphere and the photosphere. Hoekzema et al. (1998) concluded that the preferential alignment between ~3-min waves and dark photospheric intergranular lanes does not survive to the chromospheric heights; instead, there seems to be a correspondence between excess chromospheric brightness and intergranular lanes at a time delay of 2.5 min. Hoekzema et al. (2002) found that sites of enhanced wave activity in the granulation preferentially co-locate with exceptionally bright chromospheric internetwork grains, at a delay of about 2 min which might represent the sound travel time to the chromosphere. While through a statistic study, Cadavid et al. (2003) found that 72% of the G-band darkening events are followed by an enhanced chromospheric emission 2 min later; in the remaining 28% cases, the timing is reversed. Cadavid et al. (2003) also found that the G-band darkening events are usually accompanied by transient enhancement of the measured magnetic field, indicating collapse of intergranular lanes. According to Goode (2002), a collapse in the intergranular lanes can produce upward-propagating waves which subsequently lead to chromospheric brightenings.

The horizontal motions we derived in the chromosphere show a similar pattern to the photospheric supergranulation. If most chromospheric cell grains are produced by acoustic shocks, our results should indicate that the acoustic shocks are modulated by photospheric or subsurface flows. Wedemeyer et al. (2004) pointed out that convection motions play an important role in the excitation of acoustic waves. It is well known that photospheric granules tend to move in a systematic way as characterized by the supergranulation. If the collapse of intergranular lanes is really the source of acoustic waves that produce the chromospheric cell grains, we may expect a coherence between the photospheric supergranulation and the motion of the collapsing site of intergranular lanes. In other words, the collapsing site of intergranular lanes has a tendency to move with the granules. This will also naturally yield a comparable horizontal velocity in the photosphere and chromosphere.

As pointed out by Hoekzema & Rutten (1998), it is worthwhile to use photospheric flow tracking to enable studies of chromospheric response to photospheric or subsurface excitation sites while following migrations of the latter over mesoscale and larger distances. Our study focuses on the comparison between horizontal motions in the photosphere and chromosphere, and thus provide some insights into this issue. The coherent supergranule-scale behavior between motions in the two layers seems to indicate that the chromospheric cell grains mark locations where acoustic events follow on granular collapses in the evolving intergranular lanes.

It is also possible that the propagation of the shock waves is influenced by the supergranulation. The shock wave flux might

be advected by the supergranular flows toward the network while it is propagating upward from the photosphere and dissipated in the chromosphere.

However, the resolution of the TRACE data we used here is not very high. More high-resolution and high-cadence observations of different layers are needed to further study the dynamics of granular evolution in intergranular lanes and the chromospheric response (Rutten et al. 2008). And detailed 3-dimensional numerical simulation should also be done to investigate the role of granular motions in the excitation of acoustic shocks and the subsequent production of chromospheric cell grains.

5. Summary and conclusion

We have applied the highly efficient balltracking technique to TRACE images obtained in the white-light band and three UV passbands centered at 1700 Å, 1600 Å, and 1550 Å. We have demonstrated that the supergranular flow pattern in the photosphere can be recovered by applying this tracking method to the white-light images observed by TRACE. This is the first time that horizontal motions in a large quiet area of the solar chromosphere have been investigated. Our analysis revealed a striking correlation between the horizontal velocities derived in the white-light band and the UV passbands.

The interpretation of our finding is not straightforward, since we tracked the apparent motions of the chromospheric internetwork (cell) grains, the nature of which is still under debate. If the cell grains (or most of them) correspond to enhanced internetwork magnetic elements, the velocity fields revealed by TRACE UV observations should represent the horizontal component of magneto-convection in the chromosphere. Then our finding seems to provide evidence for the way on which mass and energy are supplied to the corona and solar wind at the height of the chromosphere, which is predicted or suggested by many recent observational and modeling studies. However, as believed by many authors, the cell grains may be entirely produced by acoustic shocks propagating upward to the chromosphere. If the cell grains are indeed of acoustic origin, the velocity fields revealed by our TRACE UV observations should reflect the motion pattern of the short-living chromospheric brightness as induced by acoustic shocks. Then the striking correlation between the horizontal velocities derived in the UV and white-light passbands seems to indicate that the excitation of enhanced wave activity is modulated by the photospheric granular motions, or that the shock waves are advected by the supergranular flows toward the network while it is propagating upward from the photosphere and dissipated in the chromosphere.

We conclude that it is important to investigate the role of granular motions in the excitation of shocks through numerical modeling. In addition, future high-resolution and high-cadence observations including dopplergrams, magnetograms, and imaging of the photosphere and chromosphere are needed to investigate and understand the coupling between the two layers.

We realize that our results and conclusions need to be checked and confirmed by future observations and with improved techniques. The mission of the Solar Dynamic Observatory (SDO), which was launched in February 2010, will provide full-disk high-resolution photospheric magnetograms and chromospheric images. It is likely that these data will better our understanding of the evolution of the chromospheric emission.

Acknowledgements. The TRACE satellite is a NASA small explorer mission that images the solar photosphere, transition region and corona with unprecedented spatial resolution and temporal continuity. Hui Tian and Raphael Attie are supported by the IMPRS graduate school run jointly by the Max Planck Society and the Universities of Göttingen and Braunschweig. The work of Hui Tian's group at Peking University is supported by the National Natural Science Foundation of China (NSFC) under contracts 40874090, 40931055, and 40890162. The space physics group at PKU are also supported by the Beijing Education Project XK100010404, the Fundamental Research Funds for the Central Universities, and the National Basic Research Program of China under grant G2006CB806305. We thank the anonymous referee for his/her careful reading of the paper and for the comments and suggestions.

References

Aiouaz, T. 2008, ApJ, 674, 1144
Aiouaz, T., Peter, H., & Lemaire, P. 2005, A&A, 435, 713
Axford, W. I., Mckenzie, J. F., & Sukhorukova, G. V. 1999, Space Sci. Rev., 87, 25
Attie, R., Innes, D. E., & Potts, H. E. 2009, A&A, 493, L13
Berrilli, F., Consolini, G., Pietropaolo, E., et al. 2002, A&A, 381, 253
Brandt, P. N., Rutten, R. J., Shine, R. A., & Trujillo Bueno, J. 1992, in Cool Stars, Stellar Systems, and the Sun, ed. M. S. Giampapa, & J. A. Bookbinder, ASP Conf. Ser., 26, 161
Brandt, P. N., Rutten, R. J., Shine, R. A., & Trujillo Bueno, J. 1994, in Solar Surface Magnetism, ed. R. J. Rutten, & C. J. Schrijver (Dordrecht: Kluwer), NATO ASI Series C, 433 , 251
Büchner, J., & Nikutowski, B. 2005, Proceedings of Solar Wind 11/SOHO 16, ESA SP-592, 141
Cadavid, A. C., Lawrence, J. K., Berger, T. E., & Ruzmaikin, A. 2003, ApJ, 586, 1409
Carlsson, M., & Stein, R. F. 1997, ApJ, 481, 500
Chae, J., Denker, C., Spirock, T. J., et al. 2000, Sol. Phys., 195, 333
Curdt, W., Tian, H., Dwivedi, B. N., & Marsch, E. 2008, A&A, 491, L13
Dammasch, I. E., Curdt, W., Dwivedi, B. N., & Parenti, S. 2008, Ann. Geophys., 26, 2955
Damé, L., Gouttebroze, P., & Malherbe, J.-M. 1984, A&A, 130, 331
Damé, L. 1985, in Theoretical Problems in High Resolution Solar Physics, ed. H. U. Schmidt, MPA/LPARL Workshop (München: Max-Planck-Institut für Physik und Astrophysik, MPA), 212, 244
Damé, L., & Martic, M. 1987, ApJ, 314, L15
Damé, L., & Martic, M. 1988, in Advances in Helio- and Asteroseismology, ed. J. Christensen-Dalsgaard, & S. Frandsen (Dordrecht: Reidel), IAU Symp., 123, 433
Del Moro, D., Giordano, S., & Berrilli, F. 2007, 472, 599
Deubner, F.-L. 1971, Sol. Phys., 17, 6
de Wijn, A. G., Rutten, R. J., Haverkamp, E. M. W. P., & Sütterlin, P. 2005, A&A, 441, 1183
de Wijn, A. G., Lites, B. W., Berger, T. E., et al. 2008, ApJ, 684, 1469
Dowdy, J. F. Jr., Rabin, D., & Moore, R. L. 1986, Sol. Phys., 105, 35
Foukal, P., 1978, ApJ, 223, 1046
Gabriel, A. H. 1976, Philos. Trans. R. Soc. London A, 281, 575
Giovanelli, R. G., 1980, Sol. Phys., 67, 211
Goode, P. R. 2002, BAAS, 34, 730
Goode, P., Strous, L., Rimmele, T., & Stebbins, R. 1998, ApJ, 495, L27
Handy, B. N., Acton, L. W., Kankelborg, C. C., et al. 1999, Sol. Phys., 187, 229
He, J.-S., Tu, C.-Y., & Marsch, E. 2007, A&A, 468, 307
He, J.-S., Tu, C.-Y., & Marsch, E. 2008, Sol. Phys., 250, 147
Hoekzema, N. M., & Rutten, R. J. 1998, A&A, 329, 725
Hoekzema, N. M., Rutten, R. J., Brandt, P. N., & Shine, R. A. 1998, A&A, 329, 276
Hoekzema, N. M., Rimmele, T. R., & Rutten, R. J. 2002, A&A, 390, 681
Innes, D. E., Genetelli, A., Attie, R., & Potts, H. E. 2009, A&A, 495, 319
Jin, C.-L., Wang, J.-X., & Zhao, M. 2009, ApJ, 690, 279
Kamio, S., & Kurokawa, H. 2006, A&A, 450, 351
Krijger, J. M., Rutten, R. J., Lites, B. W., et al. 2001, A&A, 379, 1052
Krijger, J. M., Roudier, T., & Rieutord, M. 2002, A&A, 387, 672
Leighton, R. B., Noyes, R. W., & Simon, G. W. 1962, ApJ, 135, 474
Lin, C.-H., Banerjee, D., O'Shea, E., & Doyle, J. G. 2006, A&A, 460, 597
Lites, B. W., Rutten, R. J., & Berger, T. E. 1999, ApJ, 517, 1013
Livingston, W. C., & Harvey, J. 1975, AAS Bull., 7, 346
Loukitcheva, M., Solanki, S. K., & White, S. M. 2009, A&A, 497, 273
Marsch, E., & Tu, C.-Y. 1997, Sol. Phys., 176, 87
Marsch, E., Tian, H., Sun, J., Curdt, W., & Wiegelmann, T. 2008, ApJ, 684, 1262
Martin, S. F. 1988, Sol. Phys., 117, 243
McAteer, R. T. J., Gallagher, P. T., Bloomfield, D. S., et al. 2004, ApJ, 602, 436
McIntosh, S. W., Davey, A. R., Hassler, D. M., et al. 2007, ApJ, 654, 650
Nindos, A., & Zirin, H. 1998, Sol. Phys., 179, 253
November, L. J. 1989, ApJ, 344, 494

November, L. J., & Simon, G. W. 1988, ApJ, 333, 427
November, L. J., Toomre, J., & Gebbie, K. B. 1979, ApJ, 227, 600
November, L. J., Toomre, J., Gebbie, K. B., & Simon, G. W. 1982, ApJ, 258, 846
Peter, H. 2001, A&A, 374,1108
Potts, H. E., & Diver, D. A. 2008, Sol. Phys., 248, 263
Potts, H. E., Barrett, R. K., & Diver, D. A. 2004, A&A, 424, 253
Potts, H. E., Khan, J. I., & Diver, D. A. 2007, Sol. Phys., 245, 55
Rast, M. P. 1999, ApJ, 524, 462
Remling, B., Deubner, F.-L., & Steffens, S. 1996, A&A, 316, 196
Rieutord, M., Roudier, T., Ludwig, H.-G., et al. 2001, A&A, 377, L14
Rimmele, T. R., Goode, P. R., Harold, E., & Stebbins, R. T. 1995, ApJ, 444, L119
Roudier, T., Rieutord, M., Malherbe, J. M., & Vigneau, J. 1999, A&A, 349, 301
Rutten, R. J., & Krijger, J. M. 2003, A&A, 407, 735
Rutten, R. J., & Uitenbroek, H. 1991, Sol. Phys., 134, 15
Rutten, R. J., de Pontieu, B., & Lites, B. W. 1999a, in High Resolution Solar Physics: Theory, Observations, and Techniques, ed. T. R. Rimmele, K. S. Balasubramaniam, & R. R. Radick, Proc. 19th NSO/Sacramento Peak Summer Workshop, ASP Conf. Ser., 183, 383
Rutten, R. J., Lites, B. W., Berger, T. E., & Shine, R. A. 1999b, in Solar and Stellar Activity: Similarities and Differences, ed. C. J. Butler, & J. G. Doyle, ASP Conf. Ser., 158, 249
Rutten, R. J., de Wijn, A. G., & Sütterlin, P. 2004, A&A, 416, 333
Rutten, R. J., van Veelen, B., & Sütterlin, P. 2008, Sol. Phys., 251, 533
Shimojo, M., & Tsuneta, S. 2009, ApJ, 706, L145
Simon, G. W., & Leighton, R. B. 1964, ApJ, 140, 1120
Simon, G. W., Title, A. M., Toska, K. P., et al. 1988, ApJ, 327, 964
Sivaraman, K. R. 1991, in Mechanisms of Chromospheric and Coronal Heating, ed. P. Ulmschneider, E. Priest, & B. Rosner, Heidelberg Conf. (Berlin: Springer Verlag), 44
Sivaraman, K. R., & Livingston, W. C. 1982, Sol. Phys., 80, 227
Sivaraman, K. R., Gupta, S. S., Livingston, W. C., et al. 2000, A&A, 363, 279
Skartlien, R., Stein, R. F., & Nordlund, Å. 2000, ApJ, 541, 468
Solanki, S. K., Lagg, A., Woch, J., Krupp, N., & Collados, M. 2004, Nature, 425, 692
Strous, L. H., Goode, P. R., & Rimmele, T. R. 2000, ApJ, 535, 1000
Tian, H., Tu, C.-Y., Marsch, E., He, J.-S., & Zhou, G.-Q. 2008a, A&A, 478, 915
Tian, H., Xia, L.-D., He, J.-S., Tan, B., & Yao, S. 2008b, Chin. J. Astron. Astrophys., 8, 732
Tian, H., Marsch, E., Curdt, W., & He, J.-S. 2009, ApJ, 704, 883
Tian, H., Tu, C.-Y., Marsch, E., He, J.-S., & Kamio, S. 2010, ApJ, 709, L88
Title, A. M., Tarbell, T. D., Topka, K. P., et al. 1989, ApJ, 336, 475
Tritschler, A., Schmidt, W., Uitenbroek, H., & Wedemeyer-Böhm, S. 2007, A&A, 462, 303
Tu, C.-Y., Zhou, C., Marsch, E., et al. 2005, Science, 308, 519
Vernazza, J. E., Avrett, E. H., & Loeser, R. 1981, ApJS, 45, 635
Wang, H. 1988, Sol. Phys., 117, 343
Wang, H., & Zirin, H. 1988, Sol. Phys., 115, 205
Wang, J., Wang, H., Tang, F., Lee, J. W., & Zirin, H. 1995, ApJ, 160, 277
Wang, Y., Noyes, R. W., Tarbell, T. D., & Title, A. M. 1995, ApJ, 447, 419
Wedemeyer, S., Freytag, B., Steffen, M., Ludwig, H.-G., & Holweger, H. 1999, A&A, 414, 1121
Worden, J., Harvey, J., & Shine, R. 1999, ApJ, 523, 450
Yang, G., Xu, Y., Wang, H., & Denker, C. 2003, ApJ, 597, 1190
Yang, S. H., Zhang, J., Jin, C. L., Li, L. P., & Duan, H. Y. 2009, A&A, 501, 745
Yi, Z., & Molowny-Horas, R. 1995, A&A, 295, 199
Zhang, J., Wang, J., Wang, H., & Zirin, H. 1998, A&A, 335, 341
Zhang, J., Ma, J., & Wang, H. 2006, ApJ, 649, 464
Zhang, M., & Zhang, H. 2000, Sol. Phys., 194, 19